this approach has yielded considerable insight into the factors that determine the energetic splittings of the δ,δ^*-derived manifold of electronic states of these species, there is clear experimental evidence that the nature of the ligands needs to be considered in order for the finer details of the $^1(\delta \rightarrow \delta^*)$ transition energy and intensity to be understood for specific classes of quadruply metal-metal bonded complexes. It has been proposed[5,16] that the majority of the intensity of the $^1(\delta \rightarrow \delta^*)$ transitions of halide-containing quadruply M-M bonded dimers is stolen from higher lying $\pi(X) \rightarrow \delta^*$ transitions that meet certain symmetry and polarization criteria and that the extent of intensity stealing should depend significantly upon both the energy gap between the $^1(\delta \rightarrow \delta^*)$ and $\pi(X) \rightarrow \delta^*$ transitions and the X-M-M angle. The $^1(\delta \rightarrow \delta^*)$ transition energy is also affected by such a charge-transfer mixing mechanism, albeit to a lesser extent. These phenomena are best illustrated by the $Mo_2X_4(PMe_3)_4$ series (X = Cl, Br, I), for which the metal-metal distance is essentially constant at ~2.13 Å: X = Cl, $\bar{\nu}_{max}$ = 17 090 cm^{-1}, ϵ_{max} = 3110 M^{-1} cm^{-1}; X = Br, $\bar{\nu}_{max}$ = 16 720 cm^{-1}, ϵ_{max} = 4060 M^{-1} cm^{-1}; X = I, $\bar{\nu}_{max}$ = 15 720, ϵ_{max} = 5150 M^{-1} cm^{-1}.[16] We would expect the complexes examined in this study to be increasingly sensitive to charge-transfer mixing in the orders $Re_2F_8^{2-}$ < $Re_2Cl_8^{2-}$ < $Re_2Br_8^{2-}$, based on optical electronegativities, and $Re_2Cl_8^{2-}$ < $Mo_2Cl_4(PMe_3)_4$, based on the Cl-M-M angle (∠Cl-Re-Re = 103°; ∠Cl-Mo-Mo = 112°),[10,20] with an increase in mixing with pressure being manifested as an anomalously red-shifted or intense $^1(\delta \rightarrow \delta^*)$ transition.

Taking this caveat on metal-ligand mixing into consideration, we believe the following conclusions can be drawn from the observed pressure dependence of the $^1(\delta \rightarrow \delta^*)$ transition. In the case of $Re_2F_8^{2-}$ (for which charge-transfer mixing should be negligible) and of $Re_2Cl_8^{2-}$ (for which charge-transfer mixing should be relatively small at low pressures), a decrease in Re-Re bond length is the dominant factor at low pressure, accounting for the initial increase in transition moment. At higher pressures, the torsion becomes dominant, and the turning point in the graph (Figure 4) indicates the pressure required for the onset of this distortion. That this turning point occurs at a higher pressure for $Re_2F_8^{2-}$ than for $Re_2Cl_8^{2-}$ suggests that shorter Re-Re distances are required before substantial twisting occurs in the fluoro complex, consistent with simple steric considerations.

The dramatic red shift of the $^1(\delta \rightarrow \delta^*)$ transition with pressure, evident in Figure 3, can be understood in terms of the pressure-induced torsional distortion discussed above for $Re_2F_8^{2-}$ and $Re_2Cl_8^{2-}$. This effect is most extreme for the bulky Br^- ligands. However, the insensitivity of the transition moment to pressure (Figure 4) cannot be explained on the basis of simple distortion arguments. Charge-transfer mixing should be more important for $Re_2Br_8^{2-}$, and it is our view that the observation of a constant intensity for the $^1(\delta \rightarrow \delta^*)$ transition with pressure indicates that this mechanism compensates for the expected decrease in transition moment (vide supra) due to pressure-induced molecular distortions.

Finally, we need to examine the hypothesis of CSD[8] that van der Waals interactions between the δ^* orbitals and the surrounding medium are the dominant factor in determining the energies of the $^1(\delta \rightarrow \delta^*)$ transitions as a function of pressure. As we noted previously,[7] the higher energy 313-nm $\pi(Cl) \rightarrow \delta^*(Re)$ charge-transfer band of $Re_2Cl_8^{2-}$ was observed merely to broaden with pressure without changing transition energy or integrated absorption moment. CSD report a similar insensitivity to pressure of the positions of the 414- and 671-nm $\pi(X) \rightarrow \delta^*$ bands of $Re_2Br_8^{2-}$ and $Re_2I_8^{2-}$, respectively.[8] If interactions between the medium and the δ^*-orbitals of the complexes were primarily responsible for the observed behavior of the $^1(\delta \rightarrow \delta^*)$ transition, it is difficult to understand why the $^1(\pi(X) \rightarrow \delta^*)$ transitions would be insensitive to pressure. We also note that our observed pressure-induced trends are not discontinuous across the fluid/crystalline phase transitions of the solvents, which again argues that the importance of solvent-solute interactions is minor.

Acknowledgment. This work was performed at Los Alamos National Laboratory under the auspices of the U.S. Department of Energy. Additional support by the National Science Foundation (Grant CHE 84-03836 at The University of Texas at Austin) and the Office of Energy Research, Division of Chemical Sciences, U.S. Department of Energy, is gratefully acknowledged. D.E.M., C.D.T., and M.D.H. also acknowledge support from the Director's Postdoctoral Fellowship Program at LANL.

Registry No. $Re_2F_8^{2-}$, 72931-84-1; $Re_2Cl_8^{2-}$, 19584-24-8; $Re_2Br_8^{2-}$, 19584-25-9; $Mo_2Cl_4(PMe_3)_4$, 67619-17-4.

Contribution from the Department of Chemistry, Northern Illinois University, DeKalb, Illinois 60115

Electronic Absorption and MCD Spectra for the Triangular Platinum(0) Complex $Pt_3(\mu\text{-}CO)_3(P(t\text{-}Bu)_3)_3$

Huey-Rong C. Jaw and W. Roy Mason*

Received October 16, 1989

Electronic absorption and magnetic circular dichroism (MCD) spectra in the UV-vis range 1.7-5.2 μm^{-1} are reported for the triangular, trinuclear $Pt_3(\mu\text{-}CO)_3(P(t\text{-}Bu)_3)_3$ complex in CH_3CN solution at room temperature. The MCD spectrum is generally better resolved than the absorption and reveals positive A or pseudo-A terms at 2.04, 2.76, 3.85, and 4.20 μm^{-1}, a negative A term at 3.18 μm^{-1}, and a negative B term at 2.27 μm^{-1}. The spectra are interpreted in the context of some recent MO calculations in terms of transitions to E′ or A_2'' D_{3h} spin-orbit states of excited configurations that are primarily metal to ligand charge transfer (MLCT) in character.

Introduction

Platinum forms an interesting class of 42-electron trinuclear complexes **1** consisting of an equilateral triangle of Pt atoms and

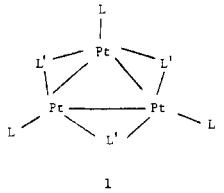

1

L′ = CO; L = $P(c\text{-}Hx)_3$[2], $P(t\text{-}Bu)_3$[3], $P(n\text{-}Bu)_3$[4], $P(CH_2CH_2CN)_3$[4]

L′ = CNR; L = CNR, R = Me, Et, t-Bu[5]

L′ = SO_2; L = PPh_3[6], $P(c\text{-}Hx)_3$[7], $P(t\text{-}Bu)_3$[7]

L′ = CS_2; L = $P(c\text{-}Hx)$[7], $P(t\text{-}Bu)_3$[7]

coplanar terminal (L) and bridging (L′) ligands.[1] The complexes have D_{3h} symmetry when the substituents on the L and L′ donor atoms are ignored, and the Pt-Pt distances are only slightly ligand

(1) For a review of complexes of type **1** and other homonuclear clusters of Pt, see: Mingos, D. M. P.; Wardle, R. W. M. *Transition Met. Chem. (London)* **1985**, *10*, 441.
(2) Albinati, A. *Inorg. Chim. Acta* **1977**, *22*, L31.
(3) Goel, R. G.; Ogini, W. O.; Srivastava, R. C. *J. Organomet. Chem.* **1981**, *214*, 405.
(4) Evans, D. G.; Hallam, M. F.; Mingos, D. M. P.; Wardle, R. W. M. *J. Chem. Soc., Dalton Trans.* **1987**, 1889.
(5) Green, M.; Howard, J. A. K.; Murray, M.; Spencer, J. L.; Stone, F. G. A. *J. Chem. Soc., Dalton Trans.* **1977**, 1509.
(6) Moody, D. C.; Ryan, R. R. *Inorg. Chem.* **1977**, *16*, 1052.

0020-1669/90/1329-3452$02.50/0

dependent and fall in the range 2.62–2.71 Å[1] (which is less than the Pt–Pt distance in Pt metal, 2.78 Å). The complexes **1** are of interest because the triangular Pt_3 unit may be visualized as a basic structural unit in larger platinum cluster molecules or a bulk metal surface, both of which have relevance to catalytic activity.[1,8] For example the $Pt_3(\mu\text{-}CO)_3(CO)_3$ unit oligomerizes into chains in the cluster anions $[Pt_3(\mu\text{-}CO)_3(CO)_3]_n^{2-}$, n = 2–5 and 10.[8] The nature of the Pt–Pt interaction and other electronic structural features in **1** and related complexes have been investigated from an extended Hückel MO viewpoint and discussed in terms of fragment molecular orbitals (FMO's).[9-11] Even allowing for the complexity of the MO schemes for complexes of the type in **1**, there is basic agreement as to the frontier orbitals, the highest occupied (HOMO's) and lowest unoccupied (LUMO's) orbitals. However, there has been virtually no experimental corroboration for these schemes, particularly from electronic spectroscopy. Therefore, in order to provide a spectroscopic basis for discussion of electronic structures of **1** and accessible low-energy excited electronic states, we report here electronic absorption and magnetic circular dichroism (MCD) spectra for $Pt_3(\mu\text{-}CO)_3(P(t\text{-}Bu)_3)_3$ in acetonitrile solution. The spectra are interpreted in the context of the recent MO models.[9-11] The $Pt_3(\mu\text{-}CO)_3(P(t\text{-}Bu)_3)_3$ complex serves as a good prototype for the complexes **1**; it is easily synthesized, is air stable in the solid and solution, and has no tendency to oligomerize in solution.

Experimental Section

The compound tris(μ-carbonyl)tris(tri-*tert*-butylphosphine)-*triangulo*-triplatinum(0), $Pt_3(\mu\text{-}CO)_3(P(t\text{-}Bu)_3)_3$, was prepared from $Pt(P(t\text{-}Bu)_3)_2$[3,12] and purified CO gas according to a literature method.[3] An orange precipitate of product formed as CO was bubbled through a pentane solution of $Pt(P(t\text{-}Bu)_3)_2$. The air-stable solid was collected by filtration, washed thoroughly with pentane and hexane, and vacuum-dried. The compound was recrystallized from CH_2Cl_2/hexane and gave satisfactory elemental analysis.

Absorption spectra were measured by using a Cary 1501 spectrophotometer. Absorption and MCD spectra were recorded simultaneously and synchronously along the same light path by means of a spectrometer described previously.[13] A magnetic field of 7.0 T was provided by a superconducting magnet system (Oxford Instruments SM2-7, fitted with a room-temperature bore tube). Spectral grade solvents were used, and all spectra were corrected for solvent blank. The solubility of $Pt_3(\mu\text{-}CO)_3(P(t\text{-}Bu)_3)_3$ in CH_3CN is low, and solutions were prepared by dissolving the solid in a few drops of CH_2Cl_2 and diluting with pure CH_3CN. The solvent blank was prepared in the same way. Spectra were also obtained for pure CH_2Cl_2 solutions, and there was very little difference between CH_2Cl_2 and CH_3CN solvents except at energies greater than 4.2 μm^{-1}, where CH_2Cl_2 absorbs strongly. Beer's law was obeyed within experimental error in the range 4×10^{-4}–5×10^{-5} M.

Results and Discussion

Electronic absorption and MCD spectra for $Pt_3(\mu\text{-}CO)_3(P(t\text{-}Bu)_3)_3$ in CH_3CN are presented in Figure 1, and quantitative spectral data are summarized in Table I. Figure 1 shows that the MCD spectrum is generally better resolved and reveals more features than the absorption spectrum. Except for bands I and III, the absorption consists of "shoulder" bands, while the corresponding MCD shows well-defined maxima and minima. The low resolution of some of the absorption bands makes the assignment of the MCD into *A* and *B* terms[14] somewhat problematic (*C* terms[14] are absent for this diamagnetic complex). However

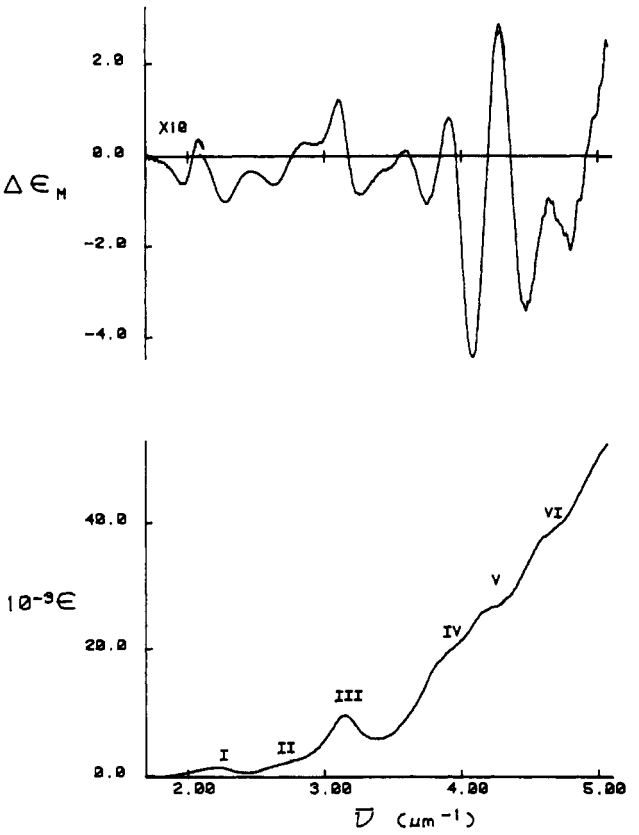

Figure 1. Electronic absorption (lower curve) and MCD (upper curve) spectra for $Pt_3(\mu\text{-}CO)_3(P(t\text{-}Bu)_3)_3$ in CH_3CN at room temperature. The MCD data for 1.8 to 2.2 μm^{-1} were multiplied by a factor of 10 before plotting. The units of $\Delta\epsilon_M$ are $(M\ cm\ T)^{-1}$.

Table I. Spectral Data for CH_3CN Solution

band no.	absorption			MCD	
	$\bar{\nu}$, μm^{-1}	λ, nm	ϵ, $(M\ cm)^{-1}$	$\bar{\nu}$, μm^{-1}	$\Delta\epsilon_M$, $(M\ cm\ T)^{-1}$
				1.97	−0.060
				b 2.04	0.0
				2.08	+0.039
I	2.20	454	1500	2.27	−1.02
				2.63	−0.64
II	2.70	370	2000[a]	*c* 2.76	0.0
				2.86	+0.36
				3.11	+1.21
III	3.15	318	9000	*b* 3.18	0.0
				3.26	−0.85
				3.59	+0.14
				3.76	−1.08
IV	3.91	256	19000[a]	*b* 3.85	0.0
				3.91	+0.86
				4.09	−4.41
V	4.20	238	25000[a]	*b* 4.20	0.0
				4.28	+2.88
				4.47	−3.39
				4.49	−1.87
VI	4.62	216	38000[a]		

[a] Shoulder. [b] *A* term. [c] Pseudo-*A* term (see text).

the data in Table I, together with Figure 1, suggest positive *A* terms are associated with bands II, IV, and V, and a negative *A* term is associated with band III. The MCD in the vicinity of band I appears to be a negative *B* term; however the MCD minimum at 2.27 μm^{-1} is shifted slightly from the absorption maximum at 2.20 μm^{-1}. This discrepancy may be partly due to an overlap of the MCD minimum with the negative part of the adjacent positive *A* term on the high-energy side. Finally, two weak MCD features appear clearly in the energy region below the maximum of band I and correspond to an unresolved low-energy tail in the absorption. Unfortunately, the lack of absorption resolution precludes definite

(7) Ritchey, J. M.; Moody, D. C. *Inorg. Chim. Acta* **1983**, *74*, 271. Ritchie, J. M.; Moody, D. C.; Ryan, R. R. *Inorg. Chem.* **1983**, *22*, 2276.
(8) Longini, G.; Chini, P. *J. Am. Chem. Soc.* **1976**, *98*, 7225. Chini, P. *J. Organomet. Chem.* **1980**, *200*, 37.
(9) Underwood, D. J.; Hoffmann, R.; Tatsumi, K.; Nakamura, A.; Yamamoto, Y. *J. Am. Chem. Soc.* **1985**, *107*, 5968.
(10) Mealli, C. *J. Am. Chem. Soc.* **1985**, *107*, 2245.
(11) Evans, D. G. *J. Organomet. Chem.* **1988**, *352*, 397.
(12) Jaw, H.-R. C.; Mason, W. R. *Inorg. Chem.* **1989**, *28*, 4370.
(13) Mason, W. R. *Anal. Chem.* **1982**, *54*, 646.
(14) For a detailed description of MCD terms as well as the theory and conventions in standard use, see: Piepho, S. B.; Schatz, P. N. *Group Theory in Spectroscopy with Applications to Magnetic Circular Dichroism*; Wiley-Interscience: New York, 1983.
(15) Pyykkö, P. *Chem. Rev.* **1988**, *88*, 563.

Table II. Excited Configurations and States

excited confgn[a]	zero-order states	spin–orbit states[b]	$\bar{A}_1/\bar{D}_0$[c]
$(2a_1')(3a_2'')$	$^1A_2''$	A_2''	
	$^3A_2''$	E'	+2
		(A_1'')	
$(3e')^3(2a_2')$	$^1E'$	E'	−2
	$^3E'$	E'	−2
		A_2''	
		(A_1'')	
		(E'')	
$(2e')^3(2a_2')$	$^1E'$	E'	+2
	$^3E'$	E'	+2
		A_2''	
		(A_1'')	
		(E'')	
$(2a_1')(4e')$	$^1E'$	E'	+1
	$^3E'$	E'	+1
		A_2''	
		(A_1'')	
		(E'')	

[a] Orbital labels as in Figure 2. Filled orbitals omitted, and symmetry-forbidden excited configurations not included. Ground-state configuration = $...(3e')^3(2a_1)^2$, $^1A_1'$. [b] Dipole-forbidden states in parentheses. [c] For E′ states using eq 1 (see text).

term assignments for these weak MCD features, but their observation provides evidence for one or more states lower in energy than the state responsible for the band I maximum.

Excited States and MCD Terms. MO calculations[9-11] predict that $Pt_3(\mu\text{-}CO)_3(P(t\text{-}Bu)_3)_3$ should be diamagnetic and have a totally symmetric ground state with a closed-shell electron configuration. The diamagnetism of the ground state has been confirmed by NMR studies.[1,3] In D_{3h} symmetry appropriate for $Pt_3(\mu\text{-}CO)_3(P(t\text{-}Bu)_3)_3$, electronic transitions from the totally symmetric $^1A_1'$ ground state are electric dipole allowed to A_2'' (out of plane, z polarized) and E′ (in plane, xy polarized) excited states. Transitions to E′ states can give rise to MCD A terms, which result from Zeeman splitting of the degenerate state by the magnetic field,[14] while transitions to both A_2'' and E′ states can show B terms, resulting from field-induced mixing of the excited states.[14] However a complication arises when two states (such as A_2'' and E′ states or two E′ states) that can interact in the presence of the field are close in energy (within their transition bandwidths). Under these circumstances the MCD may consist of two B terms of opposite sign and give the appearance of an A term (pseudo-A term).[14] Therefore an interpretation of the MCD requires a detailed knowledge of both the symmetries and relative energies of the excited states. In order to develop a suitable excited-state scheme, various low-energy excited configurations must be considered. These configurations are most easily visualized from the simplified MO energy level diagram shown in Figure 2. The most likely HOMO's and LUMO's for the Pt_3 trinuclear complex, as suggested from the MO calculations,[9-11] are included in this diagram. The important excited configurations and their associated states are listed in Table II. Excited configurations that give rise to symmetry-forbidden states $^{1,3}A_1'$, $^{1,3}A_2'$, $^{1,3}A_1''$, and $^{1,3}E''$ are not included in Table II; transitions to these states are expected to be orders of magnitude weaker than those to the symmetry-allowed E′ and A_2'' states. Since most of the orbitals of the excited configurations are based on the Pt atoms, spin–orbit interaction must be taken into account (ζ_{5d} for Pt is in the range 0.3–0.4 μm^{-1}). Table II also includes the spin–orbit states that arise from various singlet and triplet zero-order states formulated in the absence of strong spin–orbit coupling. Further, as a guide to interpreting the MCD spectrum and identifying the excitation(s) responsible for the absorption bands, the *sign* of the MCD A terms expected for the E′ states can be determined from the $\bar{A}_1/\bar{D}_0$ parameter ratio in eq 1.[14] In this equation the

$$\bar{A}_1/\bar{D}_0 = \frac{-1}{\sqrt{2}\mu_B}\langle E'||\mu||E'\rangle \qquad (1)$$

space-averaged case appropriate for nonisotropic molecules in solution is assumed, $\bar{D}_0 = {}^1/_3|\langle A_1'||\mathbf{m}||E'\rangle|^2$ is related to the dipole strength of the transition to the E′ state in question, μ_B = Bohr magnetron, and $\mu = -\mu_B(\mathbf{L} + 2\mathbf{S})$ and $\mathbf{m} = \mathbf{er}$ are the magnetic and electric moment operators, respectively. The value of $\bar{A}_1/\bar{D}_0$ for each E′ state of Table II was determined by making the standard approximation of pure 5d or 6p orbitals on Pt and neglecting two centered terms (which are assumed to be very much smaller) in the evaluation of the reduced-matrix element (RME) in eq 1. The vaues of $\bar{A}_1/\bar{D}_0$ determined in this way are collected in Table II and are based primarily on orbital symmetry properties and as such are useful in predicting A term signs, but they are probably not reliable estimates of A term magnitudes. Such magnitudes, like absorption intensities, require a complete prescription of orbital composition, which in turn would require a complete (and rigorous) MO calculation and thus would be highly model dependent.

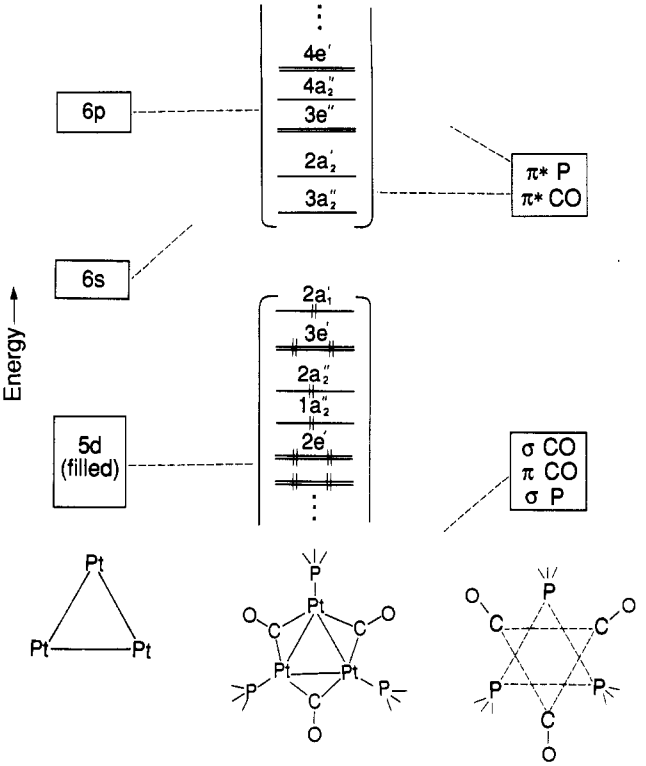

Figure 2. Schematic molecular orbital energy level diagram showing the highest energy filled orbitals and the lowest energy empty orbitals for $Pt_3(\mu\text{-}CO)_3(P(t\text{-}Bu)_3)_3$ (see refs 9–11). Orbital labels assume D_{3h} symmetry with z axis coincident with the C_3 axis.

Spectral Interpretation. On the basis of energy and the MCD B term observed, band I at 2.20 μm^{-1} is assigned as the transition to the nondegenerate A_2'' ($^1A_2''$) [$(2a_1')(3a_2'')$] state—the predominantly singlet HOMO–LUMO transition. The relatively low intensity of this band (ϵ = 1500 $M^{-1}cm^{-1}$) can be rationalized by the in-plane σ character of the $2a_1'$ orbital and the out-of-plane π character of the $3a_2''$ orbital. According to the MO calculations,[9-11] this transition should also be of the metal to ligand charge-transfer (MLCT) type because the $2a_1'$ orbital is metal localized (mostly Pt 5d) and the $3a_2''$ orbital is largely based on the CO ligands. The weak MCD features observed to the red side of band I are logically interpreted as due to spin–orbit state(s) of the $2a_1' \rightarrow 3a_2''$ excitation of predominantly triplet parentage, A_1'' and E′. However the A_1'' state is symmetry forbidden. Therefore the MCD must result from the transition to the E′ ($^3A_2''$) [$(2a_1')(3a_2'')$] state, and a positive A term is expected (see Table II). The observed MCD is consistent with a positive A term centered near 2.04 μm^{-1}; the unsymmetrical shape of the MCD in this region is interpreted as due to a coincident (negative) B term for the transition. The B terms for both the A_2'' ($^1A_2''$) and E′($^3A_2''$) states are due to mixing with higher lying states in the presence of the field and cannot result from interaction with each

other to first order because they originate from states with the same orbital functions but different spin. Unfortunately, the details of the mixing and the prediction of B term signs and magnitudes are not possible without knowing the precise nature and location of the higher lying states.

Band III at 3.15 μm^{-1} has a negative A term associated with it centered at 3.18 μm^{-1}. Of the E′ states from the lowest energy configurations in Table II only the E′ states of $(3e')^3(2a_2')$ are expected to exhibit negative A terms. On the basis of intensity, band III is assigned as the transition to E′ (^{1}E′). This transition, like the one ascribed to band I, is primarily MLCT because of the metal character of 3e′ and the ligand character of $2a_2'$. The E′ and A_2'' states of ^{3}E′ parentage are expected to lie lower in energy, and the poorly resolved absorption band II is proposed to include transitions to both of them. If these states are close in energy, as visualized here, substantial B term contributions of opposite sign are expected in the presence of the magnetic field and, as explained above, the MCD will exhibit a pseudo-A term in addition to the A term expected for the E′ (^{3}E′) state. Since the latter is predicted to be negative, the pseudo-A term must be larger and be positive to be consistent with the observed MCD for band II. In order to test this proposal the signs of the B terms from the interaction of A_2'' (^{3}E′) and E′ (^{3}E′) were estimated from their $\bar{B}_0$ parameters given in eq 2 for an $A_2''(j)$ state in the space-averaged case.[14] In eq 2 $\Delta W_{kj} = W_{E'(k)} - W_{A_2''(j)}$, the energy

$$\bar{B}_0(A_2''(j),E'(k)) = \mathrm{Re}\left[\frac{2}{3\mu_B}\sum_k \frac{1}{\Delta W_{kj}}\langle A_2''(j)||\mu||E'(k)\rangle \times \langle A_1'||\mathbf{m}||A_2''(j)\rangle\langle E'(k)||\mathbf{m}||A_1'\rangle\right] \quad (2)$$

difference between the states E′(k) and $A_2''(j)$, and the summation is over all states E′(k). The largest contribution to $\bar{B}_0$ for the A_2'' (^{3}E′) state will be from the state closest in energy, the E′ (^{3}E′) state, so that the summation can be approximated by a single term. By approximating the A_2'' (^{3}E′) and E′ (^{3}E′) states in the standard way using pure Pt 5d orbitals, we find the μ RME in eq 2 to be negative. The $\mathbf{m}$ RME's of eq 2 are more difficult to determine exactly, but overlap considerations using standard conventions[14] suggest that they should be positive. Therefore from this analysis, which is admittedly somewhat crude, we find the $\bar{B}_0$ for A_2'' (^{3}E′) at lower energy to be negative and therefore, $\bar{B}_0$ for E′ (^{3}E′) at slightly higher energy to be positive, giving a positive pseudo-A term for the pair. This result is independent of the energy ordering of the two states.[14] Therefore the MCD in the region of band II is interpreted as a large positive pseudo-A term (small ΔW between the A_2'' (^{3}E′) and E′ (^{3}E′) states), which obscures the negative A term for E′ (^{3}E′).

The higher energy shoulder absorption bands IV and V must be assigned to E′ states because of the positive A terms in the MCD spectrum. Two higher excited configurations, $(2e')^3(2a_2')$ and $(2a_1')(4e')$, give rise to E′ states that predict positive A terms (Table II). States of the former configuration are MLCT in character involving a lower energy 2e′ combination of the Pt_3 5d orbitals, while those of the later have metal-localized d → p character in that 4e′ is composed primarily of Pt_3 6p orbitals. The present results alone do not allow a decision between these two alternatives, nor is a combination of the two precluded. However the MO calculations[9-11] suggest the $(2e')^3(2a_2')$ MLCT configuration is of lower energy. Therefore bands IV and V and their MCD A terms are interpreted as transitions to the spin–orbit states E′ (^{3}E′) [$(2e')^3(2a_2')$] and E′ (^{1}E′) [$(2e')^3(2a_2')$], respectively. The ^{3}E′ state also gives an allowed A_2'' spin–orbit state, and on the basis of the same reasoning applied to band II above; a contribution from a pseudo-A term between the A_2'' (^{3}E′) and E′ (^{3}E′) states is expected if these states lie close in energy. Finally, band VI is not well resolved and the MCD appears to be complicated in this energy region, which makes a definite term assignment difficult. This band and the rising absorption to higher energy may be due to the high-energy d → p transitions, but the present results do not allow excited-state differentiation or firm confirmation.

Concluding Remarks. It is encouraging that the MCD and absorption spectra for $Pt_3(\mu\text{-}CO)_3(P(t\text{-}Bu)_3)_3$ can be reasonably interpreted in terms of the MLCT excitations from the occupied mainly 5d orbital combinations of the Pt_3 triangle to empty primarily ligand-based $3a_2''$ and $2a_2'$ orbitals described by the MO calculations.[9-11] The interpretation of the spectra advanced here however requires excited-state spin–orbit coupling be explicitly included with several prominent spectral features ascribed to transitions to states of spin-forbidden parentage. The inclusion of spin–orbit effects is standard practice when excited states and electronic spectra for molecules containing heavy atoms are described. Even though the absorption and MCD assignments provide spectroscopic support for the frontier orbitals (HOMO's and LUMO's) developed[9-11] for trinuclear Pt_3 complexes of the type in **1**, it must be admitted that the number of excited states possible is large and alternate assignments may be necessary if more accurate MO calculations become available that substantially change the energy level structure indicated in Figure 2. The assignments proposed here are considered to be the most likely because the excited configurations of Table II are expected to be lowest in energy and the transitions to the states discussed here are expected to be the most intense and therefore the most prominent in the spectra. It is interesting to note that the lowest energy MLCT excitations for the trinuclear Pt(0) complex studies here are *lower* in energy than those found for the mononuclear Pt(0) complex $Pt(P(t\text{-}Bu)_3)_2$ studied recently.[12] There the lowest energy band is found at 2.6 μm^{-1} compared to band I at 2.2 μ^{-1} and its low-energy tail extending below 2.0 μm^{-1}. This red shift of the lowest energy absorption from the mononuclear complex to the trinuclear complex is likely a reflection of the Pt–Pt interaction in the Pt_3 triangle, which will destabilize the filled 5d orbitals involved in repulsive antibonding combinations (such as 3e′ and $2a_1'$) and thus lower the energy of MLCT transitions. At the same time the bonding combinations of the 5d orbitals provide stability for the Pt_3 complex by stabilization from intermixing with 6s and 6p orbitals on the adjacent Pt centers. This intermixing is facilitated by relativistic stabilization of the 6s orbitals (and to a lesser extent the 6p orbitals) relative to 5d.[15] However the bridging CO ligands (and other L′ ligands of **1**) also appear to play a stabilizing role for the trinuclear complex.[9] As of yet, no examples of **1** without bridging ligands L′ have been isolated.

Acknowledgment is made to the donors of the Petroleum Research Fund, administered by the American Chemical Society, for support of this work.